

Retraction

Retracted: Image Processing Method Based on FGCA and Artificial Neural Network

Scientific Programming

Received 10 October 2023; Accepted 10 October 2023; Published 11 October 2023

Copyright © 2023 Scientific Programming. This is an open access article distributed under the Creative Commons Attribution License, which permits unrestricted use, distribution, and reproduction in any medium, provided the original work is properly cited.

This article has been retracted by Hindawi following an investigation undertaken by the publisher [1]. This investigation has uncovered evidence of one or more of the following indicators of systematic manipulation of the publication process:

- (1) Discrepancies in scope
- (2) Discrepancies in the description of the research reported
- (3) Discrepancies between the availability of data and the research described
- (4) Inappropriate citations
- (5) Incoherent, meaningless and/or irrelevant content included in the article
- (6) Peer-review manipulation

The presence of these indicators undermines our confidence in the integrity of the article's content and we cannot, therefore, vouch for its reliability. Please note that this notice is intended solely to alert readers that the content of this article is unreliable. We have not investigated whether authors were aware of or involved in the systematic manipulation of the publication process.

Wiley and Hindawi regrets that the usual quality checks did not identify these issues before publication and have since put additional measures in place to safeguard research integrity.

We wish to credit our own Research Integrity and Research Publishing teams and anonymous and named external researchers and research integrity experts for contributing to this investigation.

The corresponding author, as the representative of all authors, has been given the opportunity to register their agreement or disagreement to this retraction. We have kept a record of any response received.

References

- [1] S. Yuan, "Image Processing Method Based on FGCA and Artificial Neural Network," *Scientific Programming*, vol. 2022, Article ID 4360492, 11 pages, 2022.

Research Article

Image Processing Method Based on FGCA and Artificial Neural Network

Shuping Yuan 

¹The Academy of Big Data and Artificial Intelligence Anhui Xinhua University, Hefei 230088, Anhui, China

Correspondence should be addressed to Shuping Yuan; yuanshuping@axhu.edu.cn

Received 17 August 2022; Revised 22 September 2022; Accepted 29 September 2022; Published 10 October 2022

Academic Editor: M. A. Rashid Sarkar

Copyright © 2022 Shuping Yuan. This is an open access article distributed under the Creative Commons Attribution License, which permits unrestricted use, distribution, and reproduction in any medium, provided the original work is properly cited.

With the aggravation of human sub-health problems, people's demand for medical assistance is increasing. In the face of an endless stream of diseases, doctors use medical image analysis to intuitively obtain the morphological information of the affected part of the disease, which is convenient for doctors to make a more accurate assessment of the disease. The processing of medical images is essential for the treatment of people's diseases and subsequent observation and recovery. Therefore, it is necessary to pay attention to the development and innovation of image processing. With the continuous increase of diseases and the innovation and development of technology, the existing medical image processing technology still has problems such as noise and low image contrast. The application of fuzzy genetic clustering algorithms and artificial neural networks can help image processing be more accurate and perfect. In view of the above problems, this paper has carried out data analysis and research on image processing methods based on fuzzy genetic clustering algorithm (FGCA) and artificial neural network (ANN). The research results have shown that in the case of no noise and 5% salt and pepper noise, the FGCA segmentation coefficient is the largest, at 0.9756 and 0.9758, respectively, and the segmentation entropy is the smallest, at 0.0885 and 0.0925, respectively. The liver CT (Computer Tomography) image segmentation method based on DeepLab V3+ has the highest PA, MIOU value, and Dice coefficient, which are 88%, 95%, and 94%, respectively, which has laid the foundation for the innovation and development of image processing methods.

1. Introduction

With the development of computer vision technology and image processing technology in the medical field, computer technology has become the mainstream in today's medical field to replace manual analysis of medical images. Medical imaging is a technology that uses noninvasive methods to collect images of human tissues and organs. By observing the images, it is easy to determine whether the tissues and organs have lesions. Using computer-assisted doctors to analyze medical images can more intuitively obtain the morphological information of the diseased parts of the disease, which is convenient for doctors to make more accurate disease assessments. The development of medical imaging technology has facilitated doctors to make efficient and accurate judgments on patients' conditions and has also greatly promoted the development of the field of medical research. However, medical impact equipment is

accompanied by noise during data acquisition, resulting in problems such as degraded imaging quality and low image contrast. It causes trouble for doctors to diagnose patients through CT images and other operations and is not conducive to early diagnosis and treatment of patients. In order to further understand and analyze image processing methods, this paper has studied image processing methods based on FGCA and ANN.

With the development of technology and demand, people's requirements for images are gradually increasing. In recent years, many scholars have studied image processing. Chandra et al. have proposed a method for distinguishing birds by the ratio of the distance between the eyes and the beak to the beak width and combining image processing and support vector machine classification techniques [1]. Bou-tekkouk and Sahel have proposed a method for noisy color image segmentation and edge detection based on intuitionistic fuzzy hypergraphs [2]. The collection and payment

processes of most e-commerce companies are manual, requiring additional manpower to scale buyers. With the right image and pdf processing tools, this process can be automated for more efficient and cost-effective results. The focus of Arora's research has been on automated invoice processing tasks [3]. Ahmed et al. have established a recommendation algorithm based on the recommendation threshold based on the statistical features of the image [4]. Makarenko has developed an algorithm for applying digital image processing to determine the angular position of a VTOL drone's ship deck or any other flat landing surface [5]. The abovementioned works have studied image processing from various aspects. However, the above research only remains in the economic and aerospace aspects. It does not apply new techniques to study image processing. Therefore, it is necessary to study image processing methods from other dimensions as well.

Aiming at the abovementioned problems, this paper has studied image processing methods based on FGCA and ANN. These two methods have long been widely used in other fields. In order to overcome the low efficiency of fuzzy clustering and improve its performance, Jie et al. have proposed two fuzzy clustering algorithms based on an improved adaptive cytogenetic algorithm (GA) [6]. Dong et al. have proposed a fuzzy clustering method based on multi-objective GA [7]. Goyal et al. have proposed the concept of GA based on the intuition-fuzzy k-Mode method to cluster categorical data [8]. Bangalore and Tjernberg have proposed an ANN-based condition monitoring method that uses data from supervisory control and data acquisition systems [9]. Hodo et al. have introduced the classification of normal patterns and threat patterns on IoT networks. The ANN program has been validated against simulated IoT networks, and experimental results have shown an accuracy of 99.4% [10]. The above studies have demonstrated the application of FGCA and ANN in many fields, but the research and analysis of image processing is relatively lacking. Therefore, this paper has analyzed the image processing methods based on FGCA and ANN, providing a theoretical direction for its subsequent development and laying a foundation for future practical applications.

The research on image processing in this paper has been mainly based on FGCA and ANN and has explored the composition and development of image processing from a novel perspective so as to achieve innovation. In this paper, different algorithms are used for image segmentation and comparison, and the network model is used to perform segmentation experiments on different liver CT images. The result is that FGCA has shown good antinoise performance; the stability of the improved network model is stronger, and the segmentation results are better than others. The segmentation method is better. The innovation of this paper is as follows: (1) the FCM algorithm, FGCA, and hybrid algorithm are compared in simulation experiments. (2) An image segmentation study was carried out with CT images as the research object. (3) The segmentation results of liver CT images based on DeepLab V3+ and FCN, DeepLab V2, and DeepLab V3+ algorithms are compared.

2. Methods Based on FGCA and ANN

2.1. Image Processing. The three major tasks of computer vision theory are image segmentation, feature extraction, and object recognition [11, 12]. As shown in Figure 1, image segmentation is an important process in image processing. It is an important part of automatic image processing to extract objects of interest from images of various objects using various methods. Subsequent image processing methods depend on the quality of image segmentation. Therefore, image segmentation determines the ultimate success or failure of image analysis [13].

With the increasing level of computer applications, image segmentation technology has deeply penetrated into various fields in daily life [14]. As the basis of image information processing, it has been widely used in the development of image processing. Medical image segmentation is a key technology in medical image analysis and image processing. The main goal is to divide the image into several sub-regions with the same characteristics. The basic concept of the image segmentation algorithm is actually based on the discontinuity and abrupt change of the gray level of the image edge in the gray level image. When a feature is selected, the surrounding pixel value has a trend of change with the gray value of the feature point of the selected area. Therefore, the feature edge can be segmented to achieve the result of distinguishing the selected feature area [15].

2.1.1. CT Image Preprocessing. When medical imaging equipment collects data on human tissues and organs, a large number of noise signals are often introduced, which damages the details of the image and greatly reduces the quality of the image. Therefore, before analyzing CT images, processing the initial image signals collected from medical equipment would provide convenience for subsequent image research work. Table 1 shows the CT values of normal human tissues.

There are many techniques for image preprocessing, among which the processing effect of filtering would directly affect the reliability of the result, and enhancement can process the image on a macroscopic level. Interpolation operations are used when considering image details and edges. Geometric transformation techniques, scaling techniques, translation techniques, rotation techniques, etc. can all make image processing more refined.

2.1.2. CT Image Segmentation. In the development of medical imaging, the analysis and processing of images has always been a very important part and the appearance of segmentation is of great significance to it. An image segmentation algorithm is to divide the image into several regions with specific characteristics, which can extract the region of interest from a complex scene for in-depth research and analysis. Image segmentation can be defined by the concept of set in mathematics. The discontinuity of pixel gray value can be understood as the edge of the image.

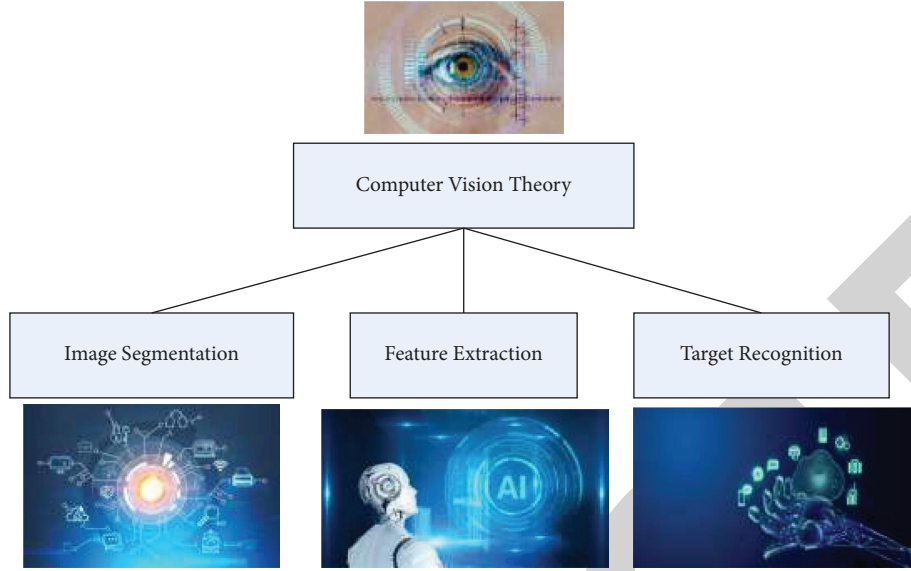


FIGURE 1: Computer vision theory.

TABLE 1: Human normal tissue CT values.

Organization	CT value
Bone tissue	200~1000
Calcification	90~300
Blood clots	65~85
Blood	15~35
Aorta	30~50
Thyroid	95~110
Liver	45~70
Kidney	45~60
Spleen	55~70
Pancreas	45~65
Lungs	-500~-900
Water	0

Therefore, the purpose of dividing the target area can be achieved by using edge segmentation. Accurately segmenting the target area of interest in the medical CT image is of great benefit to the subsequent medical diagnosis and analysis.

2.2. FGCA. Nowadays, the amount of data in various fields has grown rapidly, and its scale and capacity are beyond the scope that humans can directly process. In order to better represent and understand these information data, it is particularly important to use the processing power of the computer combined with the statistical characteristics of cluster analysis to understand it. In unsupervised classification, the analytical understanding of data is performed by searching and identifying a limited set of partitions. This unsupervised classification method is also called clustering, or unsupervised learning [16].

2.2.1. Mathematical Model of Cluster Analysis. Let the sample set be $X = \{x_1, x_2, \dots, x_m\}$; that is, the whole that needs to be classified. The sample is represented by

$x_j (j = 1, 2, \dots, m)$. If the sample has k features, it can be represented as $x_j (j = 1, 2, \dots, m)$, which is understood as the value of the j th feature of the sample x_j , where $\{x_{j1}, x_{j2}, \dots, x_{jm}\}^T \in R^m$ is called the feature vector of the sample x_j . Its constraints are expressed as

$$\begin{aligned} X_1 \cup X_2 \cup \dots \cup X_c &= X, \\ X_j \cap X_i &= \emptyset (1 \leq j \neq i \leq c). \end{aligned} \quad (1)$$

In this way, the affiliation of x_j and x_i can be expressed as

$$\beta_{ji} = \begin{cases} 1, & x_j \in X_i, \\ 0, & x_j \notin X_i. \end{cases} \quad (2)$$

Formula (2) characterizes the characteristics of hard clustering, which can also be called hard partitioning.

2.2.2. Similarity Measure. In clustering algorithms, there are many ways to measure the similarity of data samples. The most commonly used ones are the similarity coefficient method and the method based on distance measure. In the field of image segmentation, the distance between pixels is often used to describe the similarity between pixels in various regions, and then the image is segmented. The larger the distance, the smaller the correlation between the pixels, and the smaller the possibility of belonging to a category of features. Conversely, the smaller the distance, the greater the correlation between pixels, and the greater the possibility of belonging to the same category [17].

Here are some commonly used distances.

Euclidean distance is

$$d(x, y) = \sqrt{\sum_{k=1}^m (x_k - y_k)^2}. \quad (3)$$

Weighted Euclidean distance is

$$d(U_j, U_i) = \sqrt{\sum_{k=1}^m \left(\frac{U_{jk} - U_{ik}}{|x_k + y_k|} \right)^2}. \quad (4)$$

Power distance is

$$d(x, y) = \sqrt{\sum_{k=1}^m |x_k - y_k|^w}. \quad (5)$$

Mahalanobis distance is

$$d(X, Y) = \sqrt{(X - Y)^T H^{-1} (X - Y)}. \quad (6)$$

Lan distance is

$$d(x, y) = \sum_{k=1}^m \left| \frac{x_k - y_k}{x_k + y_k} \right|. \quad (7)$$

Chebyshev distance is

$$d(G_j, G_i) = \max_{k=1}^m (G_{jk} - G_{ik}). \quad (8)$$

Correlation distance is

$$\alpha_{XY} = \frac{\text{Cov}(X, Y)}{\sqrt{D(X)D(Y)}}. \quad (9)$$

Mann distance is

$$d(W_j, W_i) = \frac{1}{m} \sum_{k=1}^m |W_{jk} - W_{ik}|. \quad (10)$$

2.2.3. Clustering Algorithm. The traditional FCM algorithm is an unsupervised clustering method based on objective function optimization. The FCM algorithm is a very effective image segmentation method at present, but its defects are also very prominent. It is easy to fall into a local optimum. In addition, the FCM algorithm acts on a single pixel, ignoring the influence of the spatial neighborhood information, which makes the algorithm sensitive to noise [18].

GA is widely used in pattern recognition, function optimization, and other fields with its unique global optimization ability. The FCM algorithm based on genetic optimization can effectively solve the local optimal problem and improve the robustness of the algorithm [19].

FGCA is an improved fuzzy C-means clustering algorithm based on genetic optimization. First, a set of cluster centers close to the global optimal value is determined by GA, and then, the obtained cluster centers are used as the initial cluster centers of the FCM algorithm [20]. Since its value is close to the global optimal solution, the local search ability of the FCM algorithm itself becomes an advantage. Next, it is only necessary to find the value closest to the cluster center to determine the final global optimal solution, thus effectively avoiding the defect of falling into the local optimum.

First, the cluster center is determined by floating-point coding, which effectively reduces the complexity of the

algorithm. At the same time, in order to keep individuals as diverse as possible, the selection operation adopts the roulette selection method. The crossover probability P_a and the mutation probability P_b adaptively change with the value of the population fitness function, which can well maintain the flexibility of the GA. Moreover, the FCM algorithm that introduces spatial constraints has better robustness, which improves the image segmentation performance. The basic steps are shown in Figure 2.

The encoding is using floating-point encoding. Taking the cluster center as the gene of the chromosome, the chromosome length value is the initial cluster number d , which can be expressed as $H = \{h_1, h_2, \dots, h_d\}$. Chromosomal genes can be expressed as h_j as a floating-point number, that is the j th cluster center. After the encoding is determined, an image containing m pixels is generated in grayscale to generate M groups of real numbers, where M is the population size of GA. Each group of real numbers is d initial cluster centers randomly selected as chromosomal genes from image pixels, and the result of M random extraction is encoded according to the above-mentioned floating-point encoding method, that is, $H_{11}, H_{12}, \dots, H_{1M}$.

The main function of the fitness function value is to evaluate the evolutionary adaptability of an individual. In the FCM algorithm, the criterion for a good clustering effect is that the value of the required objective function is small. According to the constraints of the fitness function in GA, that is, the larger the function value, the stronger the individual survival ability. Using the inverse of the objective function as the fitness function, the individual fitness function defined by the FGCA algorithm is given as follows:

$$f = \frac{1}{1 + J_{FGCA}}. \quad (11)$$

The basic operation of GA mainly consists of three parts: selection, crossover, and mutation.

(1) *Selection.* The selection operation is the process of survival of the fittest in the current population. The specific operation of the roulette method is as follows: first, the 10% initial cluster centers with the highest fitness value are selected from the current population and directly retained in the next generation population. The remaining individuals are assigned the selection probability P_a according to the fitness value, as shown in the following formula:

$$P_a = q(1 - q)^{a-1}. \quad (12)$$

In the formula, q is a constant, and the general value is 0.55. a represents the initial cluster center with the remaining individual fitness values sorted as a . Roulette selection is performed according to P_a , and the corresponding initial cluster centers are found to generate the next generation of groups.

(2) *Crossover.* Two chromosomes that are paired in GA exchange some of the genes on the chromosomes in some way to form two new individuals. The encoding method is floating-point encoding, so the crossover operation adopts

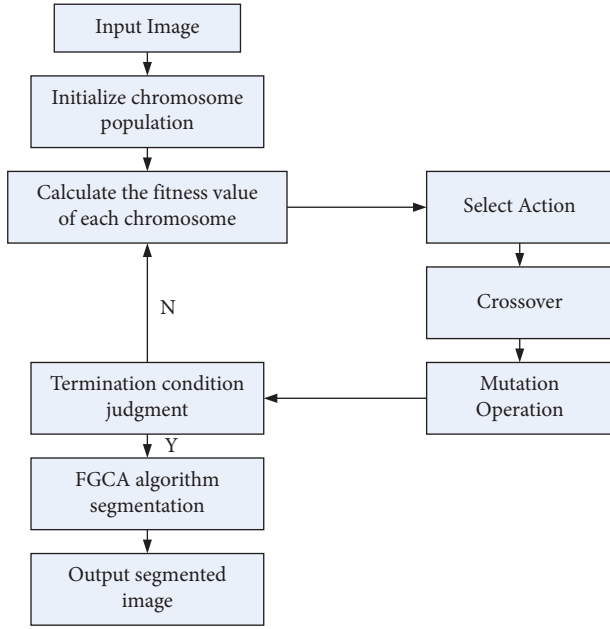


FIGURE 2: Algorithm flow.

linear single-point crossover. First, generate random numbers $t, t \in [0, 1]$. If $t \leq P$, we perform a crossover operation on this individual and select a set of chromosomes A and B for pairing. At the same time, random number $p, p \in [0, 1]$, is generated, and the linear operation shown in Figure 3 is performed on the paired chromosomes to generate two new individuals A_1, B_1 .

$$\begin{aligned} A_1 &= pA + (1 - p)B, \\ B_1 &= pB + (1 - p)A. \end{aligned} \quad (13)$$

(3) *Mutation*. Mutation is an operation that changes the value of a single or multiple bits in the individual coding structure with a small probability to generate a new individual. The mutation operation in GA is mainly completed by replacing the value of the gene in the individual chromosome code, so a random number $j, j \in [0, 1]$ is generated. When $j \in [0, 1]$, the gene value on the locus in the individual coding string is replaced with a random number or other alleles within the range to generate a new individual, as shown in Figure 4.

(4) *Control Parameter Setting*. The choice of control parameters plays a key role in GA. The quality of parameter selection directly affects the operating efficiency of GA. There is no relevant theory for the value range of the control parameters. In practical applications, multiple experiments are needed to reasonably select the control parameters. These parameters mainly include population size M , crossover probability P_a , mutation probability P_b , and maximum evolutionary algebra G_{\max} . The general recommended value range is shown in Table 2.

2.3. ANN. Since the advent of ANN, the field of deep learning has been developing. ANN imitates the movement trajectories of people's neurons and connects neurons in a

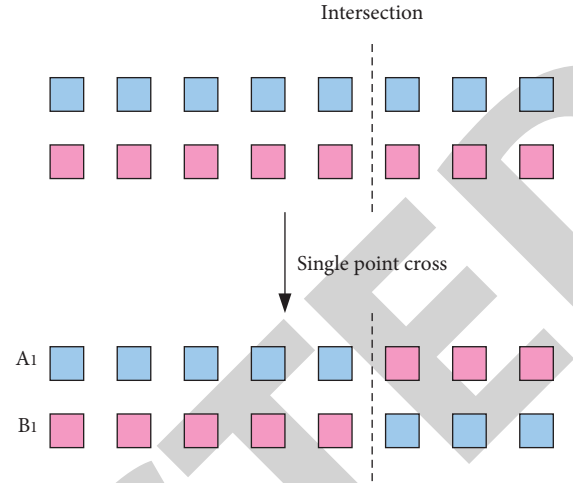


FIGURE 3: Single point crossover operation.

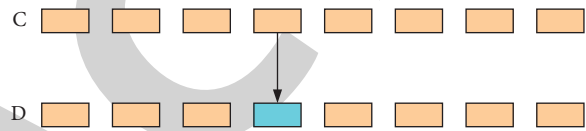


FIGURE 4: Mutation operation.

TABLE 2: Value range of control parameters.

	Control parameter	Recommended range
1	Group size M	25~100
2	Crossover probability P_a	0.5~0.99
3	Mutation probability P_b	0.001~0.2
4	Maximum evolutionary algebra G_{\max}	200~1000

certain way. It simulates the real movement of the neural network in people's brains and abstracts the received data. The essence of the convolutional neural network model is a special ANN network. Different from other neural network models, its main features are convolution operations, convolution, pooling, BN (Batch Normalization), activation functions, and fully connected layers. These form the basic structure of convolutional neural networks, which have excellent performance for large-scale image processing.

2.3.1. *Convolutional Layer*. The convolutional layer is actually a feature extraction layer that contains any number of filters, which are known as convolution kernels. Any convolution kernel can be regarded as a moving window with a size of $k \times k$. After completing the convolution operation of the convolution kernel and the corresponding sliding area, the convolution kernel and each element in the corresponding area are first multiplied and then added. Figure 5 shows a schematic diagram of a convolution operation performed on the feature map of 4×4 with a convolution kernel of 3×3 .

2.3.2. *Pooling Layer*. The pooling operation can speed up the operation and prevent the network from overfitting. There are two pooling operations, max pooling and average pooling, and

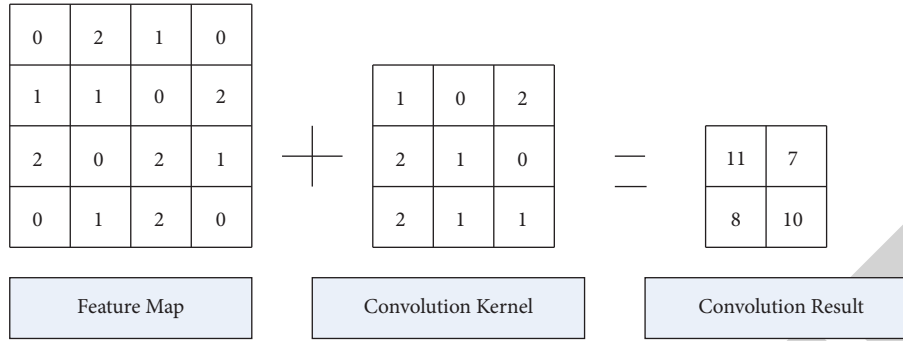


FIGURE 5: Convolution calculation process.

the process is the same for both pooling operations. The pooling kernel moves along the horizontal or vertical direction of the feature map and performs pooling processing with the corresponding location area. The maximum value of the sliding area during the window movement process is used as the maximum pooling result, and the average value of the sliding area during the window movement process is used as the average pooling result. Figure 6 is a schematic diagram of the max pooling operation. Figure 7 is a schematic diagram of the average pooling operation.

2.3.3. Activation Function Layer. In the convolutional neural network, the result of the convolution operation is linear, which provides a method for dealing with linear function problems. However, the image processing problem is a nonlinear function problem, and the activation function has nonlinear properties. Adding this to a neural network means that convolution operations can be used to deal with image problems. The neural network after processing in this way can be well used to solve difficult problems. The Sigmoid activation function is the most commonly used activation function. The functions are as follows:

$$f(x) = \frac{1}{1 + e^{-x}}. \quad (14)$$

It belongs to a kind of nonlinear mapping function. Under the mapping of this function, the linear output of the sensor can be transformed into a nonlinear output. In this way, the network can handle nonlinear problems. Sigmoid can process continuous values in the input network as 0 and 1 for output, which can effectively stabilize and optimize the output layer. However, it can cause vanishing gradient problems, and the outputs are all non-negative.

The Tanh activation function is proposed, and its function is as follows:

$$f(x) = \frac{1 - e^{-2x}}{1 + e^{-2x}}. \quad (15)$$

The output range is $(-1, 1)$, and the function mean is close to 0. When the Tanh value is 0, the Tanh convergence speed is fast. There is still the problem of vanishing gradients and the parameters cannot be updated.

Subsequently, the ReLU activation function is proposed to alleviate this problem, and the function is as follows:

$$f(x) \begin{cases} x, & x \geq 0, \\ 0, & x < 0. \end{cases} \quad (16)$$

The sigmoid activation function has two characteristics: when the input is positive, there is no defect of gradient saturation; whether it is forward propagation or reverse propagation, the calculation speed is very fast. The Tanh activation function and ReLU activation function do not have such characteristics. However, when using ReLU, some neurons are not working, causing the corresponding parameters to not be updated.

2.3.4. Batch Normalization (BN). BN is to normalize each neuron in the neuron layer, and the pure input $a^{(l)}$ of each neuron needs to be normalized. That is, data preprocessing should be done for each network layer, thereby effectively reducing the deviation of internal covariates, which can accelerate the convergence of the network. Because each layer needs to perform operations, it requires high normalized performance. Therefore, standard normalization is usually used, and each dimension of the pure input $a^{(l)}$ is processed with a standard normal distribution. The formula is as follows:

$$\hat{a}^{(l)} = \frac{a^{(l)} E[a^{(l)}]}{\sqrt{\text{var}(a^{(l)}) + \alpha}}. \quad (17)$$

Given a small batch of samples, there are K samples. The corresponding mean and variance are formulas (18) and (19), respectively:

$$\mu_D = \frac{1}{K} \sum_{k=1}^K a^{(k,l)}, \quad (18)$$

$$\varphi_D^2 = \frac{1}{K} \sum_{k=1}^K (a^{(k,l)} - \mu_D)^2. \quad (19)$$

2.3.5. Fully Connected Layer. The function of the fully connected layer is to organize, summarize, and filter the information extracted by the previous network structure, so

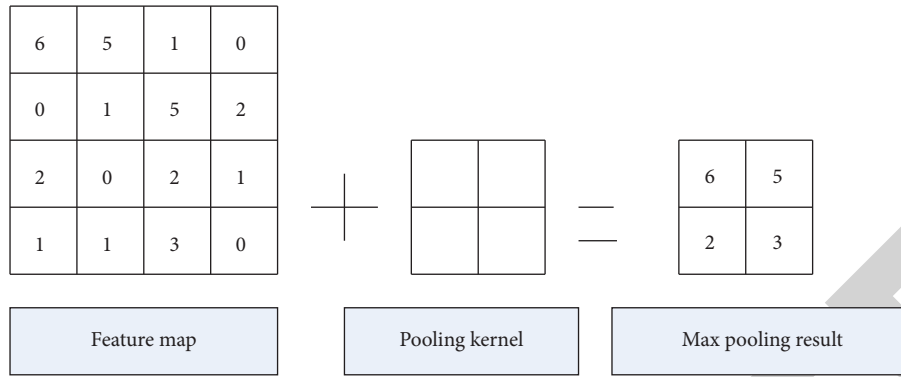


FIGURE 6: Max pooling operation.

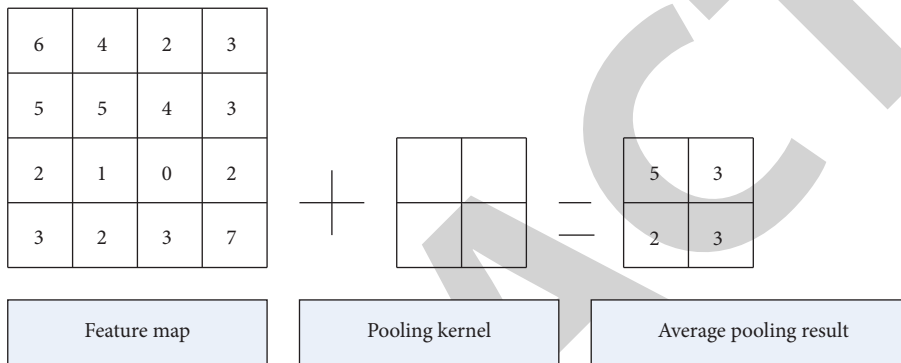


FIGURE 7: Average pooling operation.

as to obtain accurate results. The fully connected layer structure is shown in Figure 8:

2.3.6. *Commonly Used CT Image Segmentation Methods.* Fully convolutional neural network (FCN): FCN is the earliest classification network for image pixel level. FCN is mainly composed of three parts: convolution, pooling, and upsampling layers. FCN performs a “full convolution” on the network model. First, the information in the image is extracted using convolution. The size of the image is then reduced by a pooling operation. Finally, a deconvolution operation is performed to restore the size of the original image.

(1) *DeepLab V2.* When FCN is down-sampling, the receptive field of the feature map will be reduced, which may cause the image to lack some spatial information and not make full use of the full-text information in the image. Based on this, DeepLab V2 is proposed, adding the ASPP module. DeepLab V2 not only strengthens the fusion ability of multiscale information but also reduces the problem of local and global information loss [21].

(2) *DeepLab V3+.* DeepLab V3+ adopts the Encoder-Decoder-structure. The encoding structure is composed of the DCNN network and the ASPP module. The image well is downsampled by the input network for 4 times, and the

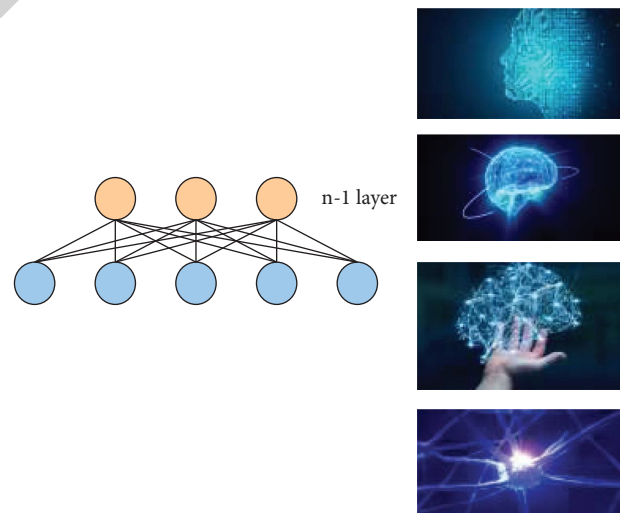


FIGURE 8: Structure diagram of the fully connected layer.

image size becomes 1/16 of the original. Image pooling is then employed to capture global information, and multiple scales capture image context. Finally, 1×1 dimension reduction operation is performed on the features output by the ASPP module to output high-level semantic features [22].

Liver CT image segmentation method based on DeepLab V3+: On the basis of Deeplab V3+, an attention model is added to enhance the ability to extract network features. At

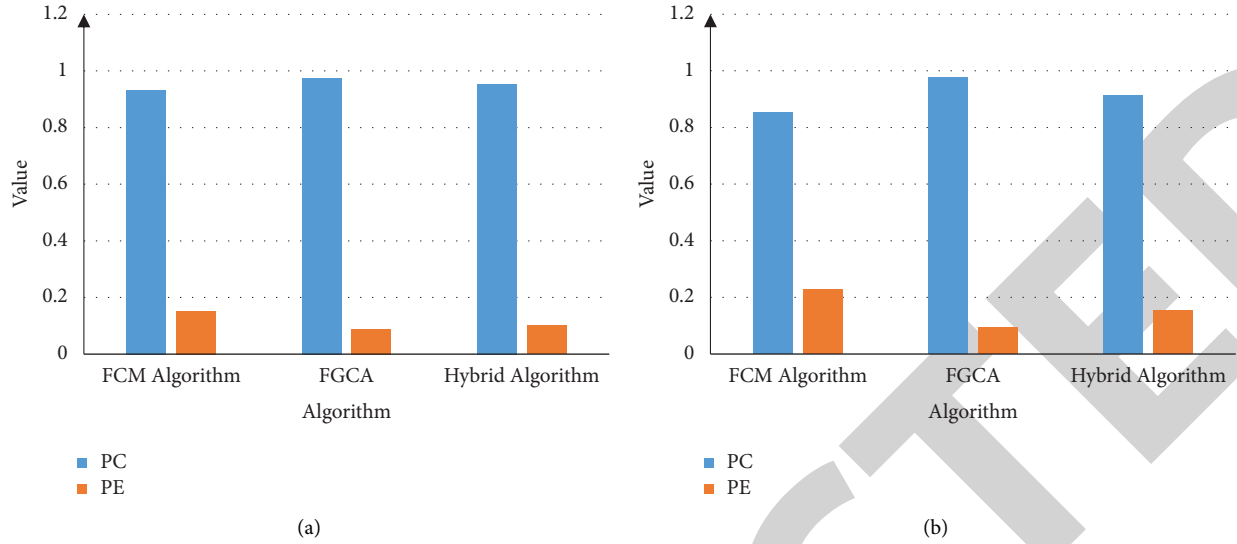


FIGURE 9: Lena image segmentation evaluation index. (a) Image segmentation evaluation index map without noise. (b) Image segmentation evaluation index map under 5% salt and pepper noise.

the same time, it also improves the ability of the network to fuse image features. Focus + CBL + CSP in the YOLOV5 network can highlight the recognition of small target tissues in the human body. Therefore, this module is used in the encoder part of DeeplabV3+ to replace the previous DCNN feature extraction module, which greatly improves the network's ability to extract image features and reduces the loss of local image information [23].

3. Image Processing Experiments

3.1. Image Processing Experiment Based on FGCA. In order to verify the performance of FGCA, this paper selects the classic lena pictures of 512×512 and uses the FCM algorithm, FGCA, and hybrid algorithm for simulation experiments and comparisons. The experimental environment is Windows7 64bit operating system, Intel(R) Core(TM) i5-3210M CPU@2.50 GHz, and memory size of 8.00 GB as well as the programming software adopts MATLAB2017b. The following non-noise lena images and lena images with 5% salt and pepper noise are separately analyzed for segmentation experiments. The experimental results are shown in Figure 9 and Table 3. PC is the segmentation coefficient, and PE is the segmentation entropy.

Figure 9(a) shows the evaluation index of image segmentation in the case of no noise. As can be seen from the figure, the maximum FGCA segmentation coefficient PC is 0.9756, and the minimum segmentation entropy PE is 0.0885. Figure 9(b) is a graph of image segmentation evaluation indicators under 5% salt and pepper noise. As can be seen from the figure, the maximum FGCA segmentation coefficient PC is 0.9758, and the minimum segmentation entropy PE is 0.0925. Among the three algorithms, FGCA shows good anti-noise performance. From Table 3, whether in the no-noise case or the 5% salt-and-pepper noise, FGCA has the smallest number of iterations, 15 and 16, respectively. Since GA optimizes the initial cluster centers, the algorithm avoids falling into a local

optimum. Therefore, the number of iterations is reduced and the convergence speed is accelerated. Meanwhile, FGCA has the longest running time among the three algorithms in both cases, 1.754 hours and 1.625 hours, respectively. The algorithm is simple, fast, robust, and effective.

3.2. Image Processing Experiment Based on ANN. The experimental operating environment used in the study is the Win10 operating system, and the experimental environment is shown in Table 4. For the study of CT segmentation images in medical images, TensorFlow is used to build a liver CT image segmentation network, and different liver CT image segmentation methods are compared.

The experiment uses the network model to train, test, and validate different liver CT images. It is proved that the proposed algorithm based on the DeepLab V3+ liver CT image segmentation method performs well in the liver CT image segmentation task. The experiment uses the image segmentation evaluation index to compare the segmentation results of the algorithm in this paper and the FCN, DeepLab V2, and DeepLab V3+ algorithms on liver CT, respectively. The evaluation results are shown in Figure 10. The PA value is the ratio of the number of correctly classified pixels to the total number of pixels in the image. The Mlou value is the ratio of the intersection of the true and expected labels to the union of the true and expected labels. The Dice coefficient is used to calculate the difference between the predicted value and the real value. It is an evaluation index in image segmentation and can solve the problem of class imbalance.

Figure 10(a) is a comparison diagram between the FCN algorithm and the algorithm in this paper. Figure 10(b) is a comparison diagram between the DeepLab V2 algorithm and the algorithm in this paper. Figure 10(c) is a comparison diagram between the DeepLab V3+ algorithm and the algorithm in this paper. Figure 10 shows the liver CT segmentation results

TABLE 3: The number of iterations and running time of each algorithm.

Noise	Algorithm	Number of fuzzy iterations	Operation hours
None	FCM	36	0.105
None	Hybrid algorithm	20	1.524
None	FGCA	15	1.754
S and P 5%	FCM	41	0.115
S and P 5%	Hybrid algorithm	20	1.524
S and P 5%	FGCA	16	1.625

TABLE 4: Experimental environment.

Serial number	Lab environment	Configuration
1	Operating system	64 bit Windows 10
2	Graphics card	GTX 1070
3	Processor	IntelCorei7- 6700 3.40 GHz
4	Deep learning framework	TensorFlow2.0

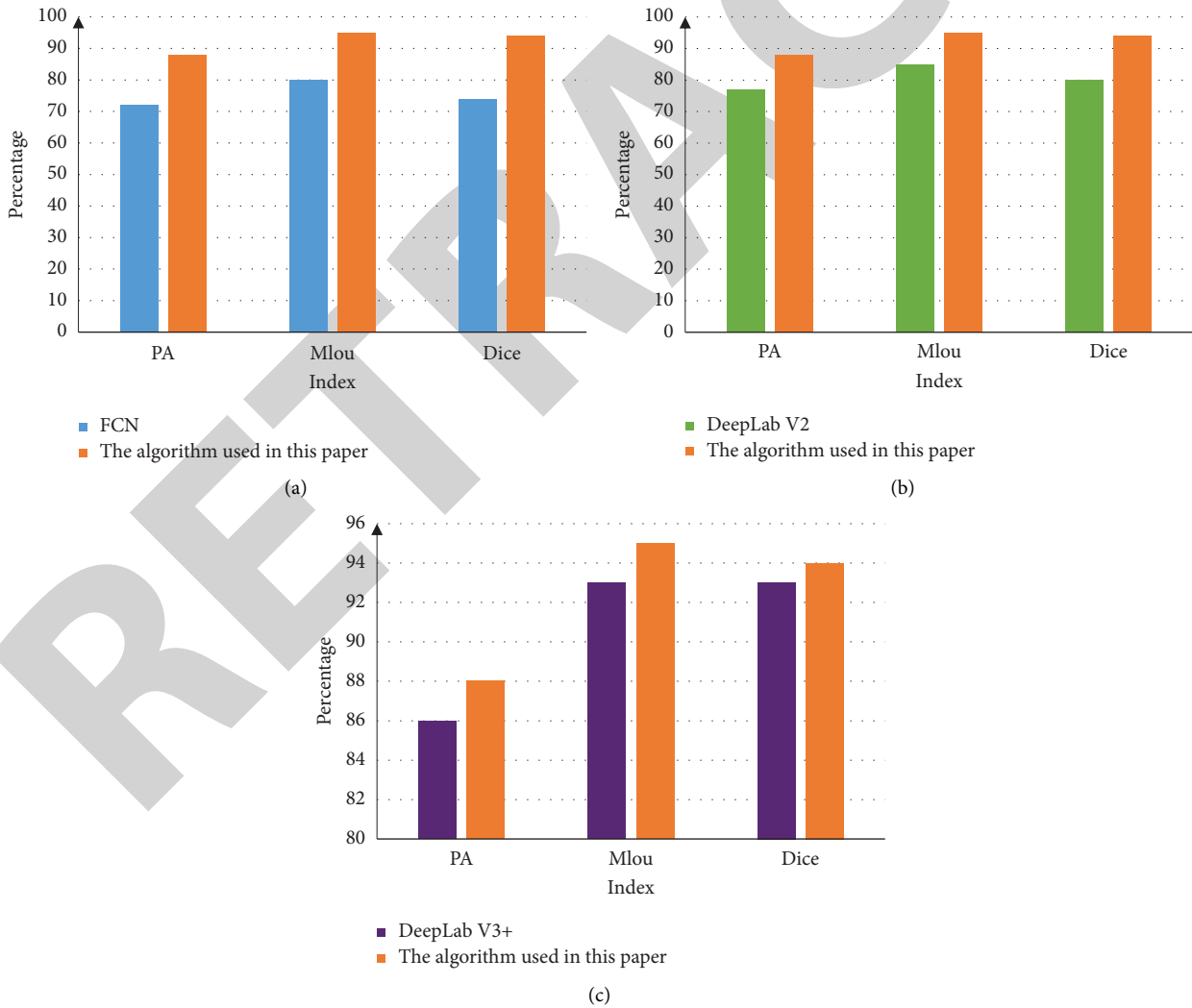


FIGURE 10: Comparison of various segmentation methods on PA, Mlou, and dice. (a) Comparison between the FCN algorithm and the algorithm in this paper. (b) Comparison between the DeepLab V2 algorithm and the algorithm in this paper. (c) Comparison between DeepLab V3+ algorithm and the algorithm in this paper.

under different segmentation networks. As can be seen from the figure, the values of the FCN algorithm are the lowest, which are 72%, 80%, and 74%, respectively. The improved model has the highest PA and MIOU values and the best Dice coefficients, which are 88%, 95%, and 94%, respectively. It shows that the real segmentation result is close to the predicted value, which confirms that the stability of the network model proposed in this paper is relatively strong and the segmentation results are better than other segmentation methods. Therefore, the improved model has more accurate and reliable segmentation results.

Compared with other methods of convolutional neural segmentation networks, the segmentation network module proposed in this paper can greatly reduce the phenomenon of repeated gradient information due to network over-optimization during the experiment. It not only effectively reduces the workload of the network but also improves the accuracy of liver CT segmentation. With the gradual increase of the network structure level, the ability of network feature fusion and extraction is also gradually improved. It is more targeted for small area tissue targets, and the feature visualization results show that this method can effectively extract detailed information about liver CT tissue areas. Moreover, the segmentation can well distinguish the boundary area, which can segment small tissue modules such as tumor liver and improve the segmentation effect of the network on small-scale targets. Compared with other cutting methods, the cutting precision is higher and the effect is better, which is of great significance for promoting the development of clinical medicine.

4. Conclusions

This paper has studied image processing methods based on FGCA and ANN, which can provide more scientific and efficient methods for image processing. Traditional image segmentation methods can only calculate low-dimensional spatial information features such as color information, shape information, and texture information of the image in the low-dimensional space of the image. Moreover, it is necessary to manually design features, and it is difficult to accurately segment the lesions in CT images. Therefore, it is very necessary to apply deep learning technology to the field of medical images, which not only transitions medical image segmentation from traditional manual segmentation to automatic segmentation but also improves the existing medical level to a certain extent. The application of FGCA alleviates the influence of noise on image quality, which is crucial for the formation of high-quality images. However, science and technology are constantly improving. In this paper, image processing has only been studied based on the most advanced technology available. It is hoped that image processing methods would continue to innovate and make breakthroughs in the future.

Data Availability

No data were used to support this study.

Conflicts of Interest

The author declares no conflicts of interest.

Authors' Contributions

The author has read the manuscript and approved for submission.

References

- [1] B. Chandra, S. K. S. Raja, R. V. Gujjar, J. Varunkumar, and A. Sudharsan, "Automated bird species recognition system based on image processing and svm classifier," *Turkish Journal of Computer and Mathematics Education (TURCO-MAT)*, vol. 12, no. 2, pp. 351–356, 2021.
- [2] F. Boutekkouk and N. Sahel, "Color image processing under uncertainty," *International Journal of Technology Diffusion*, vol. 12, no. 2, pp. 46–67, 2021.
- [3] H. Arora, "Electronic invoicing using image processing," *International Journal for Modern Trends in Science and Technology*, vol. 6, no. 12, pp. 520–523, 2021.
- [4] A. N. Ahmed, M. J. Alwazzan, and M. A. Ismael, "Study effects of pulse laser energy on human primary teeth and extraction caries area by using image processing techniques," *Neuro-Quantology*, vol. 18, no. 6, pp. 36–44, 2020.
- [5] A. A. Makarenko, "Algorithm for determining the angular position of the ship's deck from an unmanned aircraft using digital image processing," *Radio Industry (Russia)*, vol. 30, no. 4, pp. 87–97, 2020.
- [6] L. Jie, W. Liu, Z. Sun, and S. Teng, "Hybrid fuzzy clustering methods based on improved self-adaptive cellular genetic algorithm and optimal-selection-based fuzzy c-means," *Neurocomputing*, vol. 249, pp. 140–156, 2017.
- [7] Z. Dong, H. Jia, and M. Liu, "An adaptive multiobjective genetic algorithm with fuzzy c-means for automatic data clustering," *Mathematical Problems in Engineering*, vol. 2018, pp. 1–13, Article ID 6123874, 2018.
- [8] A. Goyal, P. A. Sourav, and P. Kalyanaraman, "Application of genetic algorithm based intuitionistic fuzzy k-mode for clustering categorical data," *Cybernetics and Information Technologies*, vol. 17, no. 4, pp. 99–113, 2017.
- [9] P. Bangalore and L. B. Tjernberg, "An artificial neural network approach for early fault detection of gearbox bearings," *IEEE Transactions on Smart Grid*, vol. 6, no. 2, pp. 980–987, 2015.
- [10] E. Hodo, X. Bellekens, A. Hamilton et al., "Threat analysis of IoT networks using artificial neural network intrusion detection system," *Tetrahedron Letters*, vol. 42, no. 39, pp. 6865–6867, 2017.
- [11] X. Zeng, Z. Wang, and Y. Hu, "Enabling efficient deep convolutional neural network-based sensor fusion for autonomous driving," in *Proceedings of the 59th ACM/IEEE Design Automation Conference*, San Francisco, CA, U.S.A., July 2020.
- [12] A. A. Elngar, M. Arafa, A. Fathy et al., "Image classification based on CNN: a survey," *Journal of Cybersecurity and Information Management*, vol. 6, no. 1, pp. 18–50, 2021.
- [13] R. D. Reis, V. Dravid, and S. Ribet, "Towards quantum image processing for electron microscopy," *Microscopy and Microanalysis*, vol. 27, no. S1, pp. 1348–1351, 2021.
- [14] M. A. A. Hamid, W. Alhaidari, N. A. Khan, and B. A. Usmani, "Dynamic changes of multiple sclerosis lesions on T2-FLAIR MRI using digital image processing," *International Journal of Advanced Computer Science and Applications*, vol. 11, no. 2, pp. 200–209, 2020.
- [15] P. F. Shan, "Image segmentation method based on K-mean algorithm," *EURASIP Journal on Image and Video Processing*, vol. 2018, no. 1, p. 81, 2018.

- [16] J. G. Maggay, "Mobile-based eggplant diseases recognition system using image processing techniques," *International Journal of Advanced Trends in Computer Science and Engineering*, vol. 9, pp. 182–190, 2020.
- [17] L. Shen, C. Qiu, X. Wu, and Y. Liu, "Thick plate bending and image processing algorithms assistant for deformation process discretization analyses," *Mechanics*, vol. 26, no. 5, pp. 383–389, 2020.
- [18] T. Morikawa, A. Kozakai, A. Kosugi, H. Bessho, and T. Shibahara, "Image processing analysis of oral cancer, oral potentially malignant disorders, and other oral diseases using optical instruments," *International Journal of Oral and Maxillofacial Surgery*, vol. 49, no. 4, pp. 515–521, 2020.
- [19] W. Zang, L. Ren, Z. Jiang, and X. Liu, "Modified kernel-based intuitionistic fuzzy C-means clustering method using DNA genetic algorithm," *Journal of Software Engineering*, vol. 11, no. 2, pp. 172–182, 2017.
- [20] S. K. Sahu and A. K. Shrivastava, "Analysis and comparison of clustering techniques for chronic kidney disease with genetic algorithm," *International Journal of Computer Vision and Image Processing*, vol. 8, no. 4, pp. 16–25, 2018.
- [21] N. B. Bahadure, A. K. Ray, and H. P. Thethi, "Comparative approach of MRI-based brain tumor segmentation and classification using genetic algorithm," *Journal of Digital Imaging*, vol. 31, no. 4, pp. 477–489, 2018.
- [22] A. Afram, F. J. Sharifi, A. S. Fung, and K. Raahemifar, "Artificial neural network (ANN) based model predictive control (MPC) and optimization of HVAC systems: a state of the art review and case study of a residential HVAC system," *Energy and Buildings*, vol. 141, no. APR, pp. 96–113, 2017.
- [23] J. Ongpeng, M. Soberano, A. Oreta, and S. Hirose, "Artificial neural network model using ultrasonic test results to predict compressive stress in concrete," *Computers and Concrete*, vol. 19, no. 1, pp. 59–68, 2017.